Desalination and Water Treatment
www.deswater.com

doi: 10.5004/dwt.2022.29052

278 (2022) 102–116
December

Wastewater sludge as a low-cost effective adsorbent of hexavalent chromium: equilibrium, kinetics, and thermodynamic studies

Mouna Cherifi[a,*], Wahiba Mecibah[b], Souad Bouasla[c], Debra F. Laefer[d], Sabir Hazourli[a]

[a]*Laboratory of Water Treatment and Valorization of Industrial Wastes, Chemistry Department, Faculty of Sciences Badji-Mokhtar University, Bp12, 23000 Annaba, Algeria, Tel. +213 666 54 72 85; email: cherifimim@gmail.com (M. Cherifi), Tel. +213 699 28 79 81; email: hazourlisab@yahoo.fr (S. Hazourli)*
[b]*Department of Technology, Faculty of Technology, University August 20, 1955 – Skikda, 21000 Algeria, Tel. +213 674 52 64 19; email: mecibahwahiba@yahoo.fr*
[c]*Higher School of Technological Education, Azzaba 21300, Skikda, Algeria, Tel. +213657459801; email: souad2004_chem@yahoo.fr*
[d]*Center for Urban Science and Progress and the Department of Civil and Urban Engineering, New York University, USA, email: debra.laefer@nyu.edu*

Received 25 May 2022; Accepted 17 October 2022

ABSTRACT

This manuscript demonstrates the ability to remove toxic hexavalent chromium species from aqueous solutions through adsorption in batch system using a cost-effective raw sludge (RS). The physico-chemical properties of the raw sludge were evaluated by scanning electron microscope/energy-dispersive X-ray spectroscopy, Fourier-transform infrared spectroscopy, X-ray diffraction analysis, thermogravimetric analysis, and X-ray fluorescence. The RS was found to be rich in amines and carboxylic groups, which may induce strong surface interactions with Cr(VI) ions in the solution and exhibit a porous morphology suitable for the fixation of Cr(VI) ions. The effects of adsorbent amount, contact time, initial Hexavalent chromium [Cr(VI)] concentration, pH and temperature on the adsorption of Cr(VI) were studied. Under the optimized operating conditions (initial Cr(VI) concentration = 20 mg/L, pH = 2, contact time = 60 min, temperature = 30°C) produced a maximum removal rate of 80.9% and maximum adsorption capacity of 9.84 mg/g. The equilibrium data fitted well to the Langmuir and Dubinin–Radushkevich adsorption isotherm models. The kinetic data showed good compliance with a pseudo-second-order rate model. The thermodynamic parameters indicated that the Cr(VI) removal by RS is an endothermic process with positive entropy was feasible spontaneously by an increase in the temperature. Based on the obtained results, the tested waste product sewage sludge can provide a low-cost means for the removal of Cr(VI) from synthetic effluents.

Keywords: Cr(VI); Wastewater sludge; Equilibrium data; Kinetic; Thermodynamic parameters

1. Introduction

Industrial effluents discharged in water bodies are the major source of water pollution that contribute to global water scarcity. Water contamination is a great concern to ecosystems and human health [1]. Heavy metal ions are common and challenging contaminants because of their toxic and bio-accumulative natures [2]. A highly hazardous one is hexavalent chromium [Cr(VI)], which is mainly generated from metallurgy, metal processing, leather tannery, battery industries, dyeing, and electroplating [3,4]. High exposure to Cr(VI) has been linked gastric pain, nausea, vomiting, severe diarrhea, hemorrhaging, as well as cancer in the digestive tract and lungs [5,6].

* Corresponding author.

Treatment of Cr(VI) in industrial wastewater is achievable through multiple processes including chemical reduction and precipitation [7,8], membrane filtration [9], photo-reduction [10], and electrochemical methods like electrocoagulation [11], electro-dissolution [12], electro-chemical reduction [13] and adsorption [14]. An overview of the advantages and disadvantages of these Cr(VI) removal techniques is available from Owlad et al. [15]. Prominent among these techniques, is adsorption, which has been found to be superior to other techniques for wastewater in terms of flexibility and simplicity of design, low cost, ease of operation and lack of sensitivity to toxic pollutants [16]. The most studied adsorbent for chromium is activated carbon [17], however, activated carbon is not particularly cost-effective for large-scale pollution [18]. Thus, a similar but lower cost, high-efficiency and eco-friendly adsorbent is needed. This has led to exploration of various natural and synthetic adsorbents as alternatives for chromium removal [14].

In recent years, the management of sewage sludge has become a significant issue in environmental engineering due to the enormous quantities generated and the associated disposal costs and constraints. In Algeria alone, about 550 tons of dry sludge is produced daily, and the production rate is expected to increase, because of more stringent criteria for treatment of wastewater plant effluents and the construction of new wastewater treatment plants to accommodate an increasing population. As a sustainable approach to mitigate these effects, current trends have indicated a progressive drive towards sewage sludge reuse as beneficial material [19].

Numerous research has explored using wastewater activated sludge for elimination of chromium with promising results [20–23]. Using wastewater sludge as a raw material offers the dual benefits of reduction in the sludge volume and production of an effective adsorbent with a lower cost than commercial activated carbons. However, reported use of natural sewage sludge as an adsorbent of Cr(VI) ions is less common. Gorzin et al. [24] used paper mill sludge and Qi et al. [25] used sewage sludge. Notably, sludge composition depends on several factors including wastewater origin, applied treatment, and sampling period. All directly influence the physicochemical characteristics. Consequently, current work first characterizes the available, Algerian sewage sludge via X-ray fluorescence, X-ray diffraction analysis, a scanning electron microscope, Brunauer–Emmett–Teller (BET), Fourier-transform infrared spectroscopy, thermogravimetric analysis, and point of zero charge. The second-part investigates its optimization as a low-cost adsorbent for the removal of Cr(VI) from an aqueous medium by varying initial Cr(VI) concentration, adsorbent dose, pH, contact time, and temperature. The study also provides insight into the adsorption process by mathematical modelling of the experimental isotherm, kinetic, and thermodynamic data.

2. Material and methods

2.1. Chemicals

The chemicals used in the adsorption tests include sodium chloride (NaCl), hydrogen chloride (HCl), sodium hydroxide (NaOH), sulfuric acid (H_2SO_4), 1,5-diphenylcarbazide, and potassium dichromate ($K_2Cr_2O_7$). They were purchased from Sigma-Aldrich-Fluka (Saint-Quentin, Fallavier, France).

2.2. Adsorbent preparation

The sewage sludge used in this study was collected directly from the drying beds of the Municipal Community Waste Water Treatment Plant in Annaba, Algeria. The sewage was washed repeatedly with distilled water, until neutralization and clarification of washed water was achieved. Next, the material was air dried, crushed using a mechanical grinder (Mikro-Feinmühle-Culatti L0458), sieved to a 65 μm particle size, and then dried at 105°C for 24 h. The resulting material is referred to herein as raw sludge (RS).

2.3. Adsorbent characterization

2.3.1. X-ray fluorescence

To determine qualitatively the content of metals, X-ray fluorescence (XRF) analysis was conducted with a spectrophotometer S8TIGRE Model with a tube Rh and 4 kW.

2.3.2. X-ray diffraction analysis

The examination of the RS crystal structure was undertaken through X-ray diffraction (XRD) analysis using an INEL XGR 2500 diffractometer equipped with a CPS detector 120 and a CuKα radiation source (λ = 1.5406 A). Scans were conducted from 0° to 60° at a rate of 2°min^{-1}.

2.3.3. Scanning electron microscopy and energy-dispersive X-ray spectroscopy analysis

To provide more structure and composition details of RS material, scanning electron microscopy (SEM) and energy-dispersive X-ray spectroscopy (EDS) studies were performed using SEM EDS analysis on a JEOL JSM 6390LU unit (Freising, Germany).

2.3.4. Fourier-transform infrared spectroscopy

The Fourier-transform infrared spectroscopy (FTIR) spectra of the RS were recorded on a Perkin-Elmer FTIR 1720-X spectrometer in the wave range 400–4,000 cm^{-1} with a step size of 2 cm^{-1}. The powdered samples were dispersed in KBr pellets (1/200 by weight).

2.3.5. Brunauer–Emmett–Teller

The specific surface area and pore structure was determined by using N_2 as the sorbate at –196°C with an automatic ASAP 2000 apparatus from Micrometrics. The RS was previously out-gassed at 200°C for 6 h and the specific surface area was determined by the BET method.

2.3.6. Thermogravimetric analysis

Thermogravimetric analysis (TGA) measurements were conducted using a TGA/DSC 3+ "STAR System" apparatus to monitor the mass change of the raw sludge and to monitor temperature. The 27.5 mg samples were bottom loaded

in platinum crucibles and heated from 30°C to a maximum temperature of 950°C at a constant heating rate of 5°C/min in an air atmosphere with a purge rate of 75 mL min^{-1}.

2.3.7. Point of zero charge

Point of zero charge (PZC) represents the solution pH in which the surface is neutrally charged [26], and its position defines the affinity of the surface to the ionic species [27]. The difference between the initial and final pH (pHf-pHi) was plotted against the initial pH (pHi). The term pHpzc is the point where pHf – pHi = 0.

2.4. Batch adsorption experiments

Stock solution of Cr(VI) was prepared using potassium dichromate. 1,000 mg/L of Cr(VI) solution was prepared by dissolving 2.835 g of potassium dichromate in 1 liter distilled water. Various concentrations of the solution were obtained by dilution of 1,000 mg/L of stock solution. The adsorption experiments were conducted via batch process by adding pre-specified amounts of RS to a series of beakers containing 250 mL of synthetic Cr(VI) solution of the desired concentration. The beakers were sealed and shaken at 150 rpm in an electrical water bath shaker. After adsorption equilibrium, the samples were filtered using a syringe filter, and the residual concentration of Cr(VI) in the filtrate was measured at 540 nm using a UV–Vis spectrophotometer (JENWAY 6405) via the 1.5 diphenyl carbazide standard method. The amount of Cr(VI) adsorbed per unit mass of the adsorbent (mg/g) and the percentage of Cr(VI) adsorbed were calculated using Eqs. (1) and (2), respectively:

$$q_e = \frac{\left(C_0 - C_e\right)V}{m} \tag{1}$$

$$R\left(\%\right) = \frac{C_0 - C_e}{C_0} \times 100 \tag{2}$$

where C_o and C_e are the initial and equilibrium, Cr(VI) concentrations (mg/L), respectively, V is the volume of the solution (L), and m is the weight of the adsorbent (g).

The effect of the various process parameters on the efficiency of Cr(VI) removal was investigated by varying different parameters such as initial Cr(VI) concentration (from 10 to 60 mg/L), the adsorbent mass (0.2–0.6 g), pH 2–9, and the temperature (10°C–40°C). The effect of each parameter was studied by keeping the other parameters constant.

2.5. Adsorption isotherm

The experimental equilibrium data were fitted with several isotherm models such as Langmuir, Freundlich, Temkin, Dubinin–Radushkevich, Sips, Toth, Redlich–Peterson and Hill models (each described in [28]). The expressions for those models are presented in Table 1.

2.6. Adsorption kinetics

Adsorption kinetics displays a strong relationship with the physical and/or chemical characteristics of the biochar. To further elucidate the adsorption process, the adsorption data were analyzed using four well-known kinetic models specifically pseudo-first-order, pseudo-second-order, Elovich, Boyd and intraparticle diffusion models (Table 2) [30,31].

2.7. Adsorption thermodynamics

The adsorption of Cr(VI) onto RS was investigated as a function of temperature and the thermodynamic parameters $\Delta G°$, $\Delta H°$, and $\Delta S°$, as well as activation energy (E_a), which are important in determining the feasibility, spontaneity, and the nature of adsorbate–adsorbent interactions. This was achieved using Eqs. (3)–(5):

$$\Delta G° = -RT \ln K_d \tag{3}$$

$$K_d = \frac{q_e}{C_e} \tag{4}$$

$$\ln K_d = -\frac{\Delta G°}{RT} = \frac{\Delta S°}{R} - \frac{\Delta H°}{RT} \tag{5}$$

where R is the ideal gas constant [8.314 J/(mol·K)], T is the Kelvin temperature (K), $\Delta G°$ is the Gibbs free energy change (kJ/mol), $\Delta H°$ is the enthalpy change (kJ/mol), $\Delta S°$ is the entropy change (kJ/(mol·K)), and K_d is the thermodynamic equilibrium constant.

Values of sticking probability (S^*) and activation energy (E_a) were calculated using modified the Arrhenius type equation related to surface coverage (q) shown in Eq. (6):

$$\ln\left(1-\theta\right) = \ln S^* + \frac{E_a}{RT} \tag{6}$$

$$\theta = \left(1 + \frac{C_e}{C_i}\right) \tag{7}$$

where C_e and C_i are the equilibrium and initial concentration of the adsorbate (mg/L), and q is the surface coverage.

3. Results and discussion

3.1. Adsorbent characterization

Elemental analysis of RS is shown in Table 3, the XRF results reveals that the major inorganic elements are presented as oxides. The dominant one was calcium (Ca) [39.5%], which might be attributed to the sludge hygienization with calcium carbonate ($CaCO_3$). The next largest ones were aluminum(Al) and iron (Fe) [both around 11%]. This was due to the use of aluminum sulfate [$Al_2(SO_4)_3$] and iron(III) chloride ($FeCl_3$) during treatment of the wastewater. Other detected oxides were sulfer (S), phosporous (P), potash (K) and Magnesium (Mg) but all in quantities of less than 5%. Similar results were reported by Babatunde and Zhao [35] in a wastewater sludge characterization where Al, Ca, silicon (Si), carbon (C), and Fe were also found on the adsorbent surface based XRD analysis.

The results of the XRD analysis (Fig. 1) agree with the elemental analysis in Table 3. Fig. 1 exhibits the appearance of

Table 1
List of adsorption isotherm models

Isotherm models	Linear form	Non-linear form	Applicability	References
Langmuir	$\frac{q_e}{C_e} = -K_L q_e + K_L q_m$ $\frac{1}{q_e} = \frac{1}{q_m} + \frac{1}{K_L q_m}\frac{1}{C_e}$ $\frac{C_e}{q_e} = \frac{1}{K_L q_m} + \frac{1}{q_m} C_e$ $q_e = -\frac{1}{K_L}\frac{q_e}{C_e} + q_m$ $\frac{1}{C_e} = q_m K_L \frac{1}{q_e} - K_L$	$q_e = \frac{q_m K_L C_e}{1 + K_L C_e}$	Monolayer coverage relationship formation of adsorbate molecules	[26,28]
Freundlich	$\ln q_e = \ln K_f + \frac{1}{n}\ln C_e$	$q_e = K_f C_e^{1/n}$	- Heterogeneous surface energy systems - Multilayer description adsorption with interaction between adsorbed molecules	[29]
Temkin	$q_e = B_T \ln A_T + B_T \ln C_e$	$q_e = B_t \ln\left(A_t C_e\right)$	Covers adsorbate–adsorbent interaction.	[28]
Dubinin–Radushkevich	$\ln q_e = \ln q_s - \beta\varepsilon^2$ $\varepsilon = RT\ln\left[1 + \frac{1}{C_e}\right]$ $E = \frac{1}{\sqrt{2\beta}}$	$q_e = q_s \exp\left(-K_{ad}\varepsilon^2\right)$	Adsorbate–adsorbent equilibrium relation can be expressed independently of temperature	[28]
Sips	$\ln\frac{q_e}{q_m - q_e} = \frac{1}{n}\ln C_e + \ln\left(a_s\right)^{1/n}$	$\frac{q_m a_s C_e^{1/n}}{1 + a_s C_e^{1/n}}$	- Merged Langmuir and Freundlich models - Effectively reduced to Freundlich isotherm and contradicts Henry's lawat low adsorbate concentration. - Prediction of monolayer sorption capacity based on Langmuir isotherm at high concentrations of adsorbate	[28]
Toth	$\ln\left(\frac{q_e}{K_T}\right) = \ln C_e - \frac{1}{t}\ln\left(a_T + C_e\right)$	$q_e = \frac{K_T C_e}{\left(a_t + C_e\right)^{1/t}}$	- Based on Langmuir's model with a reduced experimental error - Takes into account lateral interactions, surface heterogeneity within the system, and other deviations from ideality	[28
Hill	$\log\left(\frac{q_e}{q_{sH} - q_e}\right) = n_H \log C_e - \log K_D$	$q_e = \frac{q_{sH} C_e^{n_H}}{K_D + C_e^{n_H}}$	- Describes the binding of different species onto homogeneous substrates - This model assumes that adsorption is a cooperative phenomenon with adsorbates at one site of the adsorbent influencing different binding sites on the same adsorbent	[28]
Redlich–Peterson	$\ln\left(K_R \frac{C_e}{q_e} - 1\right) = g\ln C_e - \ln a_R$	$q_e = \frac{K_R C_e}{1 + a_R C_e^{\beta}}$	- Mix of the Langmuir and Freundlich isotherms - Redlich–Peterson isotherm equation is mainly used to explain the formation of the monolayer with multisite interaction phenomena at the same time	[27]

Table 2
List of kinetics models

Kinetic	Linear form	Plot	Parameters	References
Pseudo-first-order	$\ln(q_e - q_t) = \ln(q_e) - K_1 t$	$\ln(q_e - q_t) = f(t)$	where q_e: the amount of adsorbate in the adsorbent at equilibrium (mg/g); q_t: the amount of adsorbate in the adsorbent at time t (mg/g); K_1: constant rate of Lagergren's first-order; t: time of contact (min)	[30]
Pseudo-second-order	$\frac{t}{q_t} = \frac{1}{K_2 q_e^2} + \frac{t}{q_e}$	$\frac{t}{q_t} = f(t)$	where q_e: the amount of adsorbate in the adsorbent at equilibrium (mg/g); q_t: the amount of adsorbate in the adsorbent at time t (mg/g); K_2: constant rate of pseudo-second-order; t: time of contact (min)	[28,32]
Elovich	$q_t = \frac{1}{\beta}\ln(\alpha\beta) + \frac{1}{\beta}\ln(t)$	$q_t = f(\ln t)$	where q_t: the amount of adsorbate in the adsorbent at time t (mg/g); β: the number of sites available for adsorption; α: the initial adsorption rate (mg/g·min); t: time of contact (min)	[28,33]
Intraparticle Diffusion	$q_t = K_{ID} t^{1/2} + I$	$q_t = f(t^{1/2})$	where q_t: the amount of adsorbate in the adsorbent at time t (mg/g); K_{ID}: constant rate of intraparticle diffusion; t: time of contact (min); I: intercept of intraparticle diffusion kinetic model	[34]
Boyd	$B_t = -0.4977 - \ln\left(1 - \frac{q_t}{q_e}\right)$	$B_t = f(t)$	where B_t: Boyd constant; q_t: the amount of adsorbate in the adsorbent at time t (mg/g); q_e: the amount of adsorbate in the adsorbent at equilibrium (mg/g)	[27]

Table 3
Elemental analysis of RS

Element	CaO	SiO_2	Al_2O_3	Fe_2O_3	SO_3	P_2O_5	K_2O	MgO	TiO_2
%	39.5	24.5	11.6	11.2	4.88	2.67	1.96	1.9	0.82

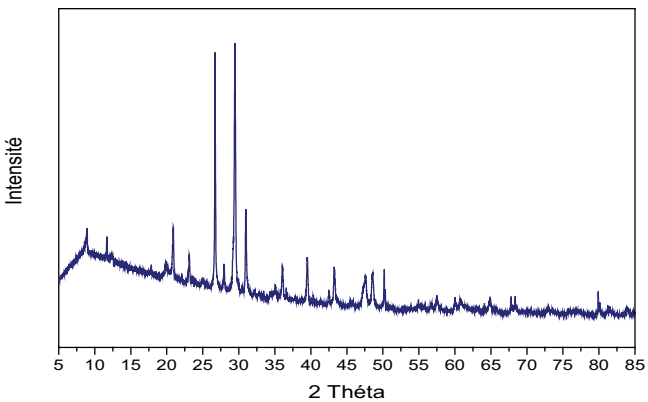

Fig. 1. XRD spectra of RS.

a solid phase crystallized with seven diffraction lines of very narrow peaks. The most intense rays correspond to quartz, Illite (KAl_2Si_3AlO)10 (OH) (10), chlorite $(Mg,Fe)_3(Si,Al)_4O_{10}(OH)_2*(Mg,Fe)_3(OH)_6$, and mansfeldite [36,37]. Some peaks denote the formation of complex oxides of Al and Fe [37,38].

The surface of the sludge observed using SEM is shown in Fig. 2. The RS surface is covered by spherical small particles, which form large agglomerates. The picture structure shows that RS is notas dense and exhibits an irregular and porous surface. This porous structure could be suitable for retention of pollutants.

EDS analysis of the RS surface indicates that RS particles consist mainly of oxygen, carbon, silicate, and aluminum. The relatively high amount of carbon may suggest that carbonates (e.g., calcium carbonates) are attached to the grain surface. The aluminum and iron oxides are attached to the surface of the silica grains. Notably, the mineralogical compositions correlate with the mineral composition highlighted by the XRF (Table 2).

The FTIR spectra of RS were used to determine the vibration frequency changes in functional groups and are displayed as a series of sorption peaks (Fig. 3). The broad sorption peak at 3,317 cm^{-1} is indicative of the existence of a bonded hydroxyl group [39]. The sorption peak around 2,927 cm^{-1} was assigned to C–H stretching [39]. The peak at 1,620 cm^{-1} represents a chelated form of the carbonyl from the carboxyl group [39]. The amine group is present at NH_2 at 23,558.28 cm^{-1}. The peak at 1,646.24 cm^{-1} corresponds to C=C ring stretching [40]. A strong, broad peak at 1,422 cm^{-1} corresponds to aliphatic and aromatic (C–H) vibrations in the planar deformation of methyl, methylene and methoxy groups [39]. The peaks observed at 1,049 and 870 cm^{-1} may be attributable to hydroxyl bending vibrations and to C–O stretching of carboxylate ions, alcoholic groups and aromatic compounds [40,41].

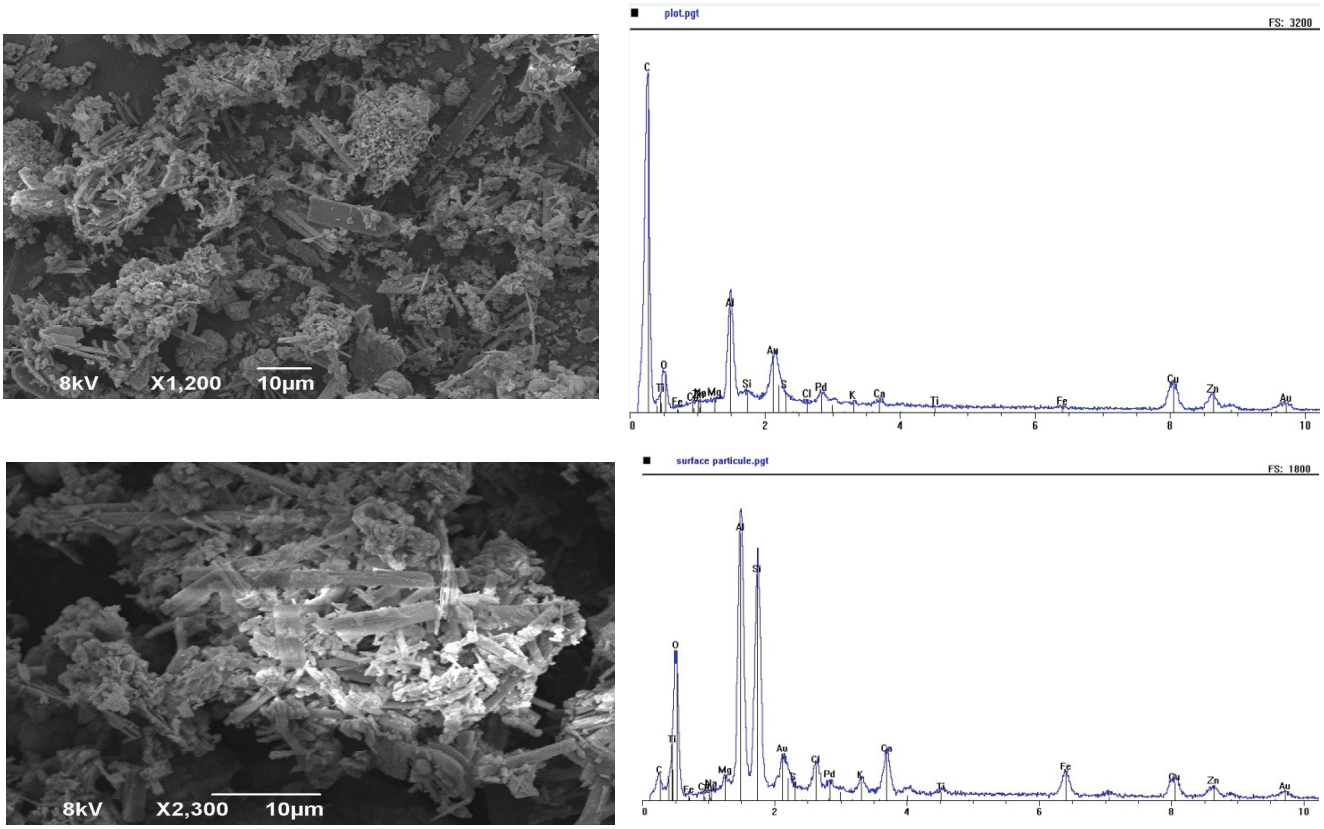

Fig. 2. SEM images of RS surface and results of EDS analysis.

The results of the BET specific surface area exhibit a surface area of 7.111 m^2/g and a pore diameter of 2.13 (Å) [mesoporous type according to International Union of Pure and Applied Chemistry (IUPAC)] [42]. According to Hu et al. [43], the presence of more meso/macro pores enhances the adsorptive capacity of adsorbent material. Importantly, the specific area value of RS powder in this study is greater than the values reported in the literature [44,45], which signifies a much higher adsorption capacity than expected. Concurrently, the specific surface area of the activated adsorbent based on wastewater sludge is also much higher than raw sludges [46,47].

The TGA analysis demonstrated changes in physico-chemical properties of the material, its decomposition, volume variation, and structural alteration when subjected to thermal treatment [48]. These are shown in Fig. 4. As the temperature rises, thermal decomposition of RS powder at different steps occurred to varying degrees through a multi-step decomposition. In the first step (<250°C), a gradual weight loss occurred until the temperature approached 250°C due to the evaporation of absorbed water [49]. Starting around 250°C the weight loss rate was faster, until the temperature neared 750°C. The accelerated weight loss was caused by (1) the breaking down of C–O and C–C bonds with the release of large amounts of CO_2 [49]; (2) the transformation reaction of aliphatic compounds, protein, and carbohydrate compounds in the sludge; (3) the breaking of peptide bonds and branched chains; and (4) the release of a large number of volatiles [50]. Finally, at temperatures above 700°C), all residual organic salts were removed, thereby corresponding to the total decomposition of RS powder.

The PZC of RW is shown in Fig. 5. The value of pH_{PZC} of RS powder was 7.05 implying a positive charge at lower values and a negative charge at higher owns. Hence, at pH values below the PZC, the groups –OH, –COOH, and $–NH_2$ protonate become positively charged, thus increasing the attraction of Cr(VI) ions with negative charge, thereby significantly fostering the adsorption process.

3.2. Adsorption and removal of Cr(VI)

3.2.1. Effects of initial concentration and contact time

The equilibrium time plays a key role in the design of cost-effective wastewater treatment systems [51]. To study this effect and the impact of the initial concentration of Cr(VI), different concentrations of Cr(VI) solution (10, 20, 40 and 60 mg/L) were each tested in 250 mL of synthetic solutions. The experiments were conducted using a fixed adsorbent mass of 0.5 g at ambient temperature (20°C), with a fixed pH (pH = 2) for a test duration of 120 min. During the experiments, samples were taken to determine the equilibrium time required. Subsequently, the Cr(VI) content in the supernatant was analyzed. Increasing chromium solution concentrations from 10 to 60 mg/L decreased the removal rate (R%) (Fig. 6). The maximum removal rate of 91.30% was achieved at 10 mg/L. At lower concentrations, the number of Cr(VI) ions to the abundant

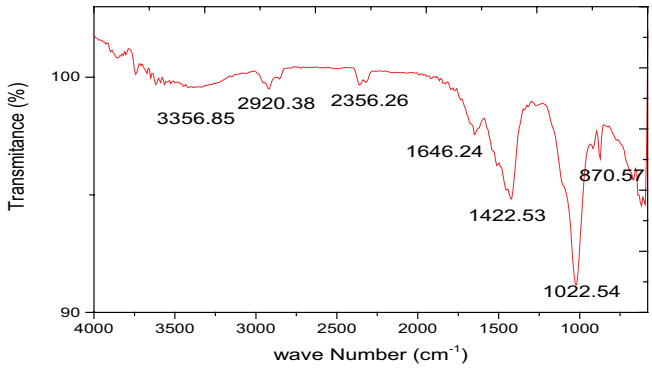

Fig. 3. FTIR spectra of RS.

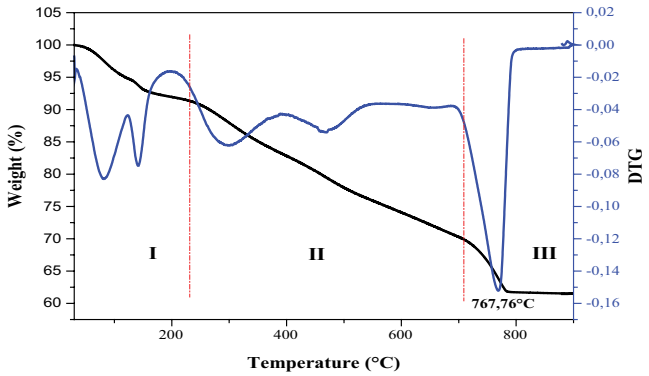

Fig. 4. TGA analysis of RS.

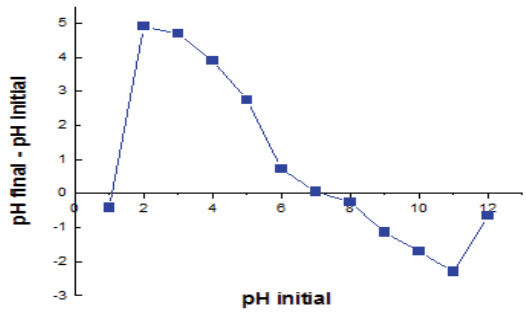

Fig. 5. Point of zero charge of RS.

active sites on the adsorbent surface was too low. Salleh et al. [52] previously established that adsorption capacity could be augmented prior to reaching saturation under the same operating conditions, where removal of 20 mg/L of Cr(VI) had a higher removal percentage (80.41%) and even higher adsorption capacity (Q = 9.849 mg/g). In addition, the high adsorption efficiency can be understood with respect to the porous nature and the specific surface area of RS. In addition, functional groups such as amine and carboxyl groups present in RS can react with Cr(VI) ions, which results in better fixation on its surface. Little difference was seen in cases of 40 and 60 mg/L, which produced in Q = 7.991 and Q = 7.17 mg/g, respectively. Kakavandi et al. [53] explained that a higher concentration gradient of Cr(VI) accelerated the mass transfer between the solid

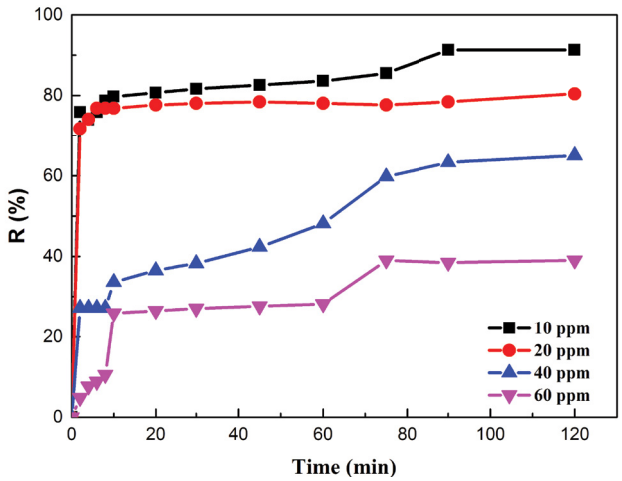

Fig. 6. Effects of concentration and contact time on Cr(VI) adsorption onto RS.

and solution and promoted the generation of precipitation, which could block the electron transfer and reduce removal efficiency.

Notably, with small concentrations (10 and 20 mg/L) of Cr(VI), the fixation of Cr(VI) into RS occurred rapidly – within the first 10 min. Higher Cr(VI) concentrations required longer times until a stationary phase was reached. Mezenner et al. [54] and Ho et al. [55] explained that in the initial treatment stage, adsorption is rapid because of the large availability of adsorption sites. After 90 min there was no significant increase in the removal rate. This, a reaction time of 90 min was selected as the optimum value for future experiments.

3.2.2. Adsorbent dosage

The effect of the RS amount was tested for levels 0.2–0.6 g for 20 mg/L concentration of Cr(VI) at 20°C for 90 min and an initial pH 2 (Fig. 7). The removal increased with higher adsorbent doses due to the greater availability of the exchangeable sites and, thus, surface area, thereby facilitating the interaction with Cr(VI) ions and consequently adsorption [56]. The highest achieved removal rate was 79.04% at the dose of 0.5 g. Higher doses did not appreciably change the rate removal. Arias et al. [57] attributed this to an overabundance of active sites potentially exceeding the demand when the adsorption process reaches saturation. Therefore, for all further experiments, the adsorbent mass was fixed at 0.5 g.

3.2.3. Effect of pH

The pH of the solution is a significant parameter in the adsorption process optimization, as it affects not only the nature of the adsorbent active site, but also the degree of ionization of the adsorbate species [58]. The most probable Ct (VI) species in aqueous solution are $Cr_2O_7^{2-}$, CrO_4^{2-}, H_2CrO_4, and $HCrO_4^-$. Their relative distribution depends on the solution's pH and Cr(VI) concentration (Fig. 8). They exist as the following oxyanions: $Cr_2O_7^{2-}$ in strongly acidic

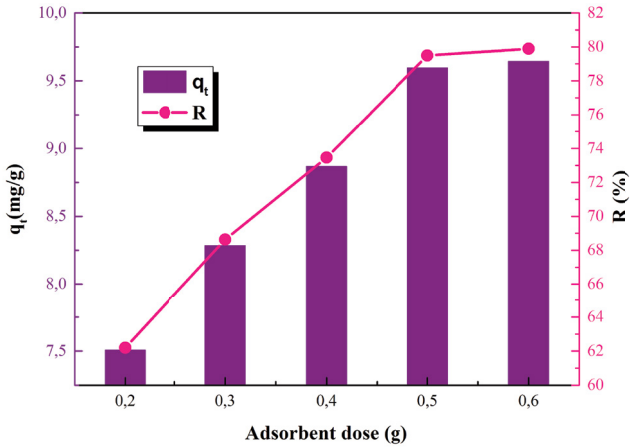

Fig. 7. Effect of adsorbent dose on Cr(VI) removal onto RS.

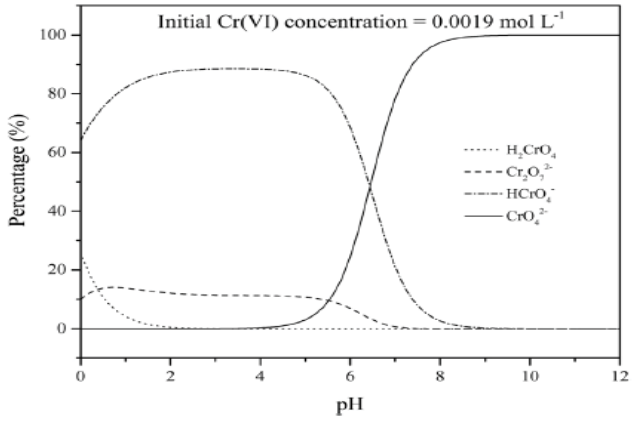

Fig. 8. Distribution diagram of chromic species according to Cr(VI) concentration and pH [59].

medium (pH < 1), $HCrO_4^-$ in acidic environment (2 ≤ pH ≤ 6), and CrO_4^{2-} in neutral and alkaline conditions (pH > 6) [59].

The effect of pH was studied in the range of 2 to 9 for a concentration of 20 mg/L of Cr(VI) during 90 min at 20°C, as illustrated in Fig. 9. In most cases, Cr(VI) removal is favored at a pH lower than the adsorbent surface "pHpzc". PZC of the RS was found to be approximately pH = 7.05 (Fig. 5). Below that value, the adsorbent surface protonated and showed a positive net charge, thus easily attracting the negative Cr(VI) ions. This revealed that the Cr(VI) removal diminished with a rise in pH, and that the maximum removal rate of 79.04% was achieved with a pH of around 2. At that pH value, Cr(VI) exists in the form of $HCrO_4^-$, and the active sites on the adsorbent become positively charged due to the excess amount of H^+ ions, which causes a strong attraction between these sites and negatively charged $HCrO_4^-$ ions. Consequently, adsorption capacity increases with a decrease of the pH solution. The electrostatic attraction decreased gradually due to the attenuation of the protonation with the increase in pH from 2 to 7.5, leading to a decline in the removal of Cr(VI). After pH > 7.05, the surface of the RS was charged negatively, and the electrostatic attraction between RS and $HCrO_4^-$ disappeared. Similar results in the adsorption of Cr(VI) were reported by previous researchers [60,61]. The amounts of adsorbed Cr(VI) may be increased, if the RS is protonated in pretreatment with an acid – assuming that the RS is a typical organic complex mainly presenting a negative surface charge which was not particularly favorable for Cr(VI) sorption [62]. Previously, Wu et al. [62] showed that 1 g of a protonated sludge at a pH of 1 reduced Cr(VI) by 20.4% compared to raw sludge through a combination of: (i) sorption of Cr(VI) onto the biomass surface, (ii) reduction of Cr(VI) to Cr(III) by surface functional groups, and (iii) release of the converted Cr(III), or and (vi) sorption to various functional groups of the biomass depending on environmental factors like pH.

Li et al [21] demonstrated that the main oxygen-containing functional groups (–OH, C–O, C=O) present in the surface of pyrolyzed sludge played an important role in adsorbing Cr(VI) and reducing it to Cr(III) at a low pH. In the study herein, Cr(VI) reduction to Cr(III) is not probable

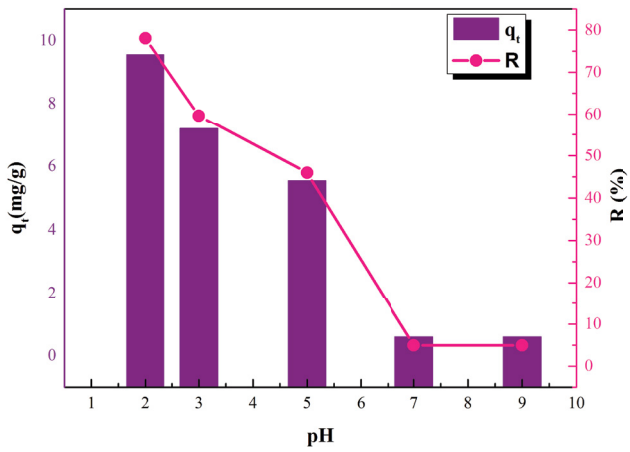

Fig. 9. Effect of the pH medium on the Cr(VI) removal in RS.

due to the limited H^+ available for the Cr(VI) reduction, but the contribution of oxygen containing functional groups is probable. So, in this study the optimum pH solution was set at 2. This corresponds to the environment of Cr(VI) in natural liquid discharges [63].

3.2.4. Effect of temperature

Temperature is an important parameter in the real applications of adsorbents. In this study, four temperatures were explored (10°C, 20°C, 30°C and 40°C) for the adsorption of 20 mg/L in the operating conditions: adsorbent dose = 0.5 g and pH = 2. The removal efficiency for Cr(VI) increased as the temperature rose (Fig. 10). The most significant gain was achieved when the temperature was increased from 10°C to 20°C when efficiency removal passed from 58.12% to 79.49%. More moderate gains were achieved with further temperature rises (80.9% at 30°C and 81.11% at 40°C). This suggests that the adsorption process of Cr(VI) onto RS is endothermic in nature. The slightly better (although not particularly cost-effective) removal

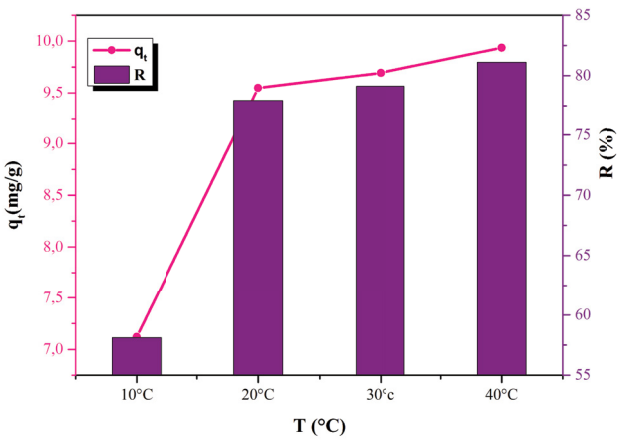

Fig. 10. Effect of temperature between 10°C and 40°C for Cr(VI) ion removal in RS.

rates at temperatures beyond 20°C may be attributed to the enhanced mobility of metal cations and the increase in the number of active sites. This is because an increasing number of cations can obtain the energy required to interact with active sites on the surface of the adsorbent. Previously, Li et al. [64] reported greater adsorption by the swelling effect within the internal structure of the adsorbent when the temperature of the aqueous solution increased.

3.3. Adsorption isotherms

Adsorption isotherms describe the relationship between the amount of adsorbed ion on the adsorbent and the final ion concentration in the solution [65]. Experimental results were analyzed using a quartet of two-parameter isotherm models including Freundlich, Langmuir, Temkin, and Dubinin–Radushkevich [66] and four more three-parameter adsorption isotherm models including the Redlich–Peterson,

Table 4
Equilibrium constants and error functions for Cr(VI) adsorption onto RS

	Two-parameter models		Three-parameter models	
	Linear	Non-linear		Non-linear
Freundlich			Sips	
K_f	5.536	6.407	q_m	11.184
n	4.444	6.134	a_S	1.143
R^2	0.727	0.862	n	1.188
RMSE	2.318	2.106	R^2	0.756
χ^2	1.151	1.225	RMSE	2.355
			χ^2	0.782
Langmuir			Toth	
K_L	3.521	6.111	K_T	25.504
q_m	10.141	10.378	a_T	2.686
R^2	0.996	0.990	t	0.803
R_L	0.014		R^2	0.999
RMSE	1.103	0.991	RMSE	0.049
χ^2	0.245	0.229	χ^2	0.000
Temkin			Hill	
A_T	42.024	42.029	q_{sh}	10.344
B_T	1.581	1.581	K_d	0.943
R^2	0.581	0.895	n_H	2.113
RMSE	1.839	1.839	R^2	0.947
χ^2	0.825	0.825	RMSE	0.653
			χ^2	0.041
Dubinin–Radushkevich			Redlich–Peterson	
q_m	10.414	10.418	K_R	6.799
β	0.2E-6		a_R	0.355
E (kJ/mol)	1.581	0.676	g	1.175
R^2	0.991	0.993	R^2	0.999
RMSE	0.591	0.473	RMSE	0.096
χ^2	0.099	0.043	χ^2	0.000

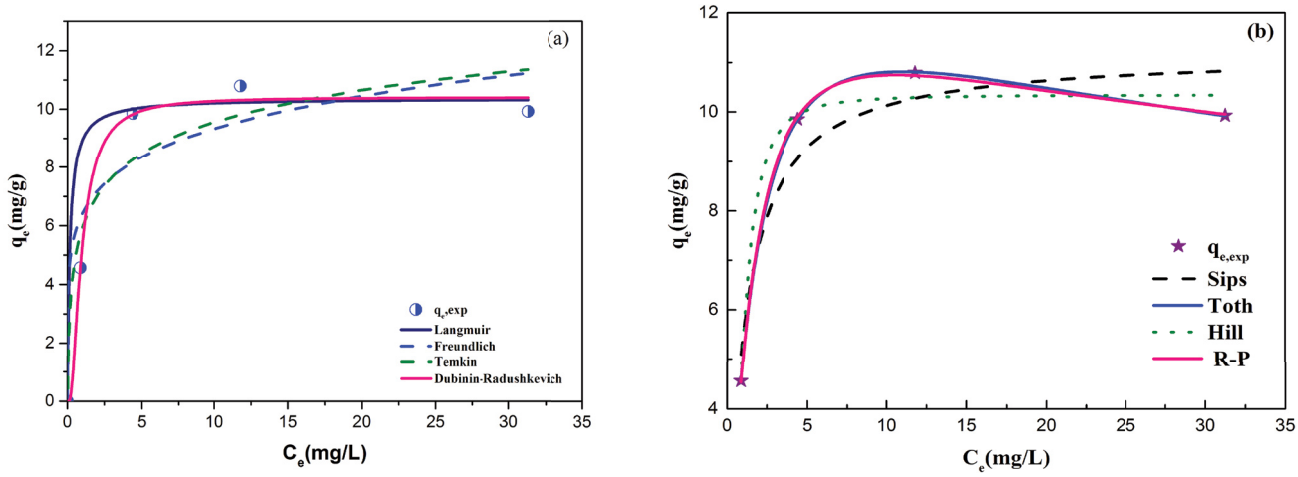

Fig. 11. Isotherm models at 20°C (a) two-parameters isotherms and (b) three-parameter isotherms.

Table 5
Kinetic parameters for Cr(VI) adsorption onto RS

	10	20	40	60
$q_{e,exp}$ (mg/g)	4.565	9.849	10.791	9.927
Pseudo-first-order				
q_e (mg/g)	0.760	3.662	8.318	9.019
K_1 (min^{-1})	0.012	0.097	0.029	0.036
R^2	0.909	0.478	0.854	0.807
RMSE	12.022	22.668	9.090	4.635
χ^2	36.263	54.978	11.822	3.743
Pseudo-second-order				
q_e (mg/g)	4.545	9.746	11.286	9.927
K_2 (g/mg·min)	0.386	0.052	1.149	1.728
R^2	0.997	0.999	0.957	0.961
RMSE	0.602	0.433	4.726	3.599
χ^2	0.664	0.020	4.238	2.038
Elovich				
B (g/mg)	5.197	5.595	0.607	0.442
α (mg/g·min)	15.81E+6	7.82E+20	5.192	1.587
R^2	0.851	0.771	0.843	0.897
RMSE	0.315	0.433	3.161	3.404
χ^2	0.030	0.020	1.538	2.495

Sips, Toth and Hill isotherm models [67]. Fig. 11 illustrates the two- and three-parameter isotherm models fitted to the experimental data at 20°C.

The isotherm parameters with correlation coefficients (R^2) and the error analyses for two and three-parameter models for Cr(VI) adsorption on RS are presented in Table 4. Amongst the various two-parameter isotherm models, the Dubinin–Radushkevich and Langmuir models achieved very strong correlations with R^2 values of 0.990 and 0.993, respectively. Among the three-parameter isotherms, the best representation of the experimental results of the adsorption was obtained using the Redlich–Peterson and Toth models since they show the minimum error values and maximum regression coefficients (Table 4).

Both R_L and n_F values indicated that the adsorption of Cr(VI) was favorable when $1 < n_F < 10$ and $0 < R_L < 1$. The maximum adsorption capacity, q_m, was determined with Langmuir and Sips models (q_m = 10.378 and 11.184 mg/g, respectively) [68].

3.4. Kinetic studies

In this study, the pseudo-first-order kinetics [69], pseudo-second-order kinetics [70], Elovich [71], intraparticle

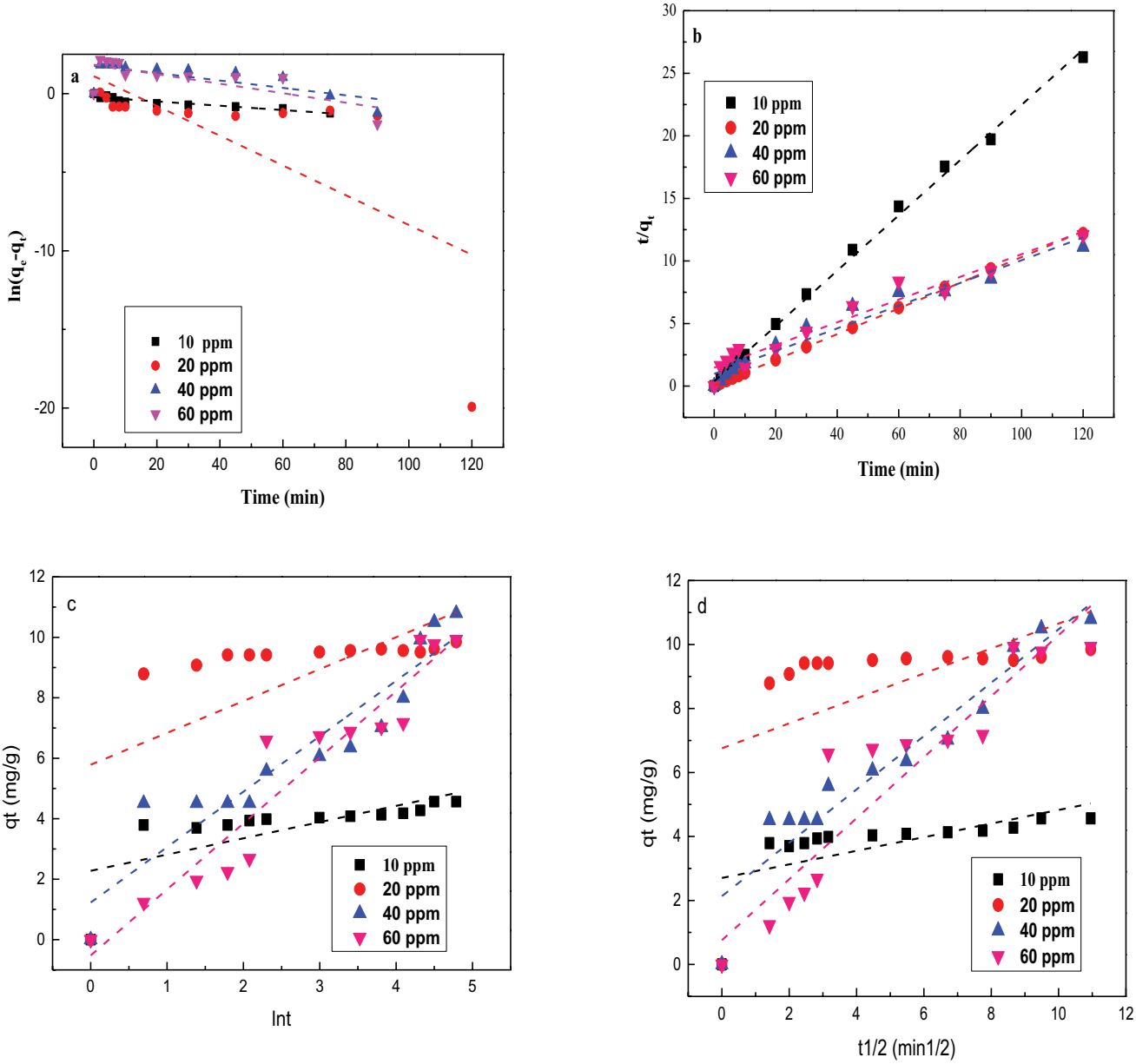

Fig. 12. Kinetic models fit for Cr(VI) adsorption onto RS, (a):pseudo first order model, (b): pseudo second order model, (c): Elovich model and (d): intraparticle diffusion model

diffusion [67,72] and Boyd models [73] were selected to discuss the kinetics of Cr(VI) removal from RS. Their details are shown in Tables 5 and 6.

The R^2 for pseudo-second-order (0.957–0.999) are higher than those obtained for pseudo-first-order (0.478–0.909) and Elovich (0.771–0.897). The values of the error functions (χ^2, RMSE) for pseudo-second-order were also lower than pseudo-first-order and Elovich, where lower values indicate smaller experimental errors. Lastly, the calculated q_e ($q_{e,\text{cal}}$) and the experimental q_e ($q_{e,\text{exp}}$), values from pseudo-second-order were very close. Therefore, based on the values of R^2, error functions, and the good agreements between $q_{e,\text{cal}}$ and $q_{e,\text{exp}}$, the pseudo-second-order model can be considered the best fitted for the experimental data.

As such, an intraparticle diffusion model was applied to investigate the mechanism of mass transport and to determine the rate controlling step during Cr(VI) adsorption on the surface of RS. Since the plots (Fig. 11) of the intraparticle diffusion did not pass through the origin, this indicates that the adsorption processes not only followed the intraparticle diffusion but that film diffusion also played an important role in both of the studied adsorption processes. These observations support the close fitting of the pseudo-second-order model. The role that film diffusion played in the adsorption processes suggests that this was mainly by covalent bonding by the surface acidic functional groups [74,75]. The Boyd model can be used to investigate whether the adsorption occurs within the pores

(particle diffusion) or occurs at the external surface (film diffusion) [76,77]. According to this model, the plot of B_t against t will yield a straight line passing through the origin, if the adsorption is governed by particle diffusion. Otherwise, the process is controlled by film diffusion [78], which appears to be the case herein (Table 6).

3.5. Thermodynamics studies

Thermodynamic parameters were evaluated to confirm the adsorption nature of the present study. The results are summarized in Table 7, which indicates that at a low temperature (10°C), Cr(VI) adsorption is not spontaneous, which is contrary to what occurs at 20°C–40°C, Also, $\Delta G°$ values were found to be negative and occurring through a spontaneous process. Decreases in $\Delta G°$ with an increase in temperature suggests that great Cr(VI) adsorption occurs at higher temperatures. The positive value of $\Delta H°$ confirms the endothermic nature of the Cr(VI) adsorption process. The magnitude of $\Delta H°$ may provide insights about the type of the adsorption process. According to the literature [68], if enthalpy change is higher than 40 kJ/mol, the process is chemisorption, which includes strong electrostatic chemical bonding between chromium ions and adsorbent surface. In contrast, when enthalpy change is less than 40 kJ/mol, adsorption is physisorption. In this work, the value of $\Delta H°$ was found to be positive and around 26.884 kJ/mol, which indicates an endothermic process that is physical in nature. The positive value of entropy change ($\Delta S°$ = 0.094) revealed the affinity of RS for Cr(VI) and increased randomness at the solid–aqueous solution interface during the adsorption. Moreover, the positive value of the energy activation (E_a = 19.283 kJ/mol) confirms the endothermicity of the adsorption process [69].

4. Comparison with published studies

Table 8 appraises the adsorption performance of Cr(VI) removal from simulated or real effluents by natural and modified adsorbents base on waste water treatment sludge. Physico-chemical properties of sludge established using XRF, XRD, SEM and revealed that sludge can have different compositions and that the related structural properties depend on the origin of the treated wastewater, as well as the origin of the waste from which this sludge comes, and that both must be considered to assess its suitability for rapid, cost-effective Cr(VI) removal. Studies reported in the literature (Table 8) demonstrated that a coal prepared by the pyrolysis of sludge provided an excellent way to reuse raw sludge as a valuable material for wastewater treatment due

Table 6
Mechanistic model parameters for Cr(VI) adsorption

Cr(V) (mg/L)	10	20	40	60
Intraparticle diffusion model				
K_{diff} (mg/g·min$^{1/2}$)	0.083	0.067	0.732	0.917
C (mg/g)	3.630	9.076	2.867	1.017
R^2	0.920	0.626	0.954	0.845
Boyd model				
Intercept	1.294	2.378	–0.237	–0.401
R^2	0.909	0.501	0.854	0.807

Table 7
Mechanistic model parameters for Cr(VI) adsorption

Cr(VI)				
T (K)	$\Delta G°$ (kJ/mol)	$\Delta H°$ (kJ/mol)	$\Delta S°$ (kJ/mol)	E_a (kJ/mol)
283	0.219			
293	–0.722	26.884	0.094	19.283
303	–1.664			
313	–2.606			

Table 8
Removal efficiencies and adsorption capacities of Cr(VI) onto sludge-based adsorbents

Adsorbent	Q (mg/g) R (%)	Initial Cr(VI)	Optimum conditions	References
Red sludge modified by lanthanum	17.35 mg/g	40 mg/L	pH = 7, dose = 4 g/L, t = 180 min	[17]
Sludge impregnated + $FeCl_3$ + $ZnCl_2$ + pyrolysis at 550°C	65 mg/g	50 mg/L	pH = 2, dose = 0.2 g/L, t = 360 min	[18]
- Raw sludge	R = 81%	100 mg/L	pH = 2, dose = 4 g/L, t = 360 min	[20]
- Sludge + H_2SO_4 + pyrolysis 650°C	R = 99.61%			
Paper mill sludge + impregnation + $ZnCl_2$	23.18 mg/g 84.72%	50 mg/L	pH = 4, dose = 3.5 g/L, t = 180 min	[24]
NZVI + raw sludge	11.56 mg/g	50 mg/L	pH = 2, dose = 4 g/L, t = 1,440 min	[83]
- Polyethyleneimine modified activated sludge	86.96 mg/g	101.2 mg/L	pH = 5, dose = 2 g/L, t = 40 min	[84]
Sludge pyrolysis at 900°C	17.46 mg/g		Low pH	[21]
- Raw sludge	R = 69%		Neutral medium	[25]
- Steel slag + pyrolysis	R = 99.75%			
Raw sludge	9.5 mg/g 79.04%	20 mg/L	pH = 2, 2 g/L, t = 90 min	This study

to the evolution of its textural properties. The modification of the sludge surface by chemical treatment like the incorporation of the element such as iron and $ZnCl_2$, better enhanced the removal efficiency. Specifically, in addition to physical adsorption and electrostatic interactions phenomena like redox, chelation and doping adsorption were found to be the main mechanisms for the adsorption of Cr(VI) and that the removal rate of Cr(VI) could reach 100%. However, Ying et al. [79] demonstrated that while pyrolysis of raw material can enhance the surface area, the adsorption of Cr(VI) is not necessarily improved.

Absorbents prepared from raw sludge tested in this study showed relatively high removal yield and reduction or precipitation operation is helpful to eliminate completely chromium, herein [5,7] to meet the effluent limits imposed by local environmental legislation. The raw sludge is simple to employ, readily accessible, and inexpensive, as no additives or pyrolysis processes are necessary. Furthermore, chromium could be recovered from sludge after adsorption by either chemical or electrochemical methods with economic conditions [11,80] or chromic smudge could be valorized in several fields like an adsorbent for the removal of pollutants of water [81,82].

5. Conclusions

The present investigation shows the potential of a wastewater raw sludge (RS) as a low-cost effective material for Cr(VI) removal from aqueous solution by adsorption in a batch system. According to the findings in this paper, the following conclusions can be drawn:

- Raw sludge is characterized by its porous structural aspects, which suitable for removing Cr(IV), BET surface area relatively higher than other sludges, and high thermal resistance. The main components corresponding to XRD analysis are CaO, SiO_2, Al_2O_3, and Fe_2O_3. The FTIR spectrum uncovered a large number of functional groups, including amine and carboxylic groups, which played important roles in adsorbing Cr(VI) at low pH levels.
- The waste material raw sludge was demonstrated to have the potential to remove 80.90% of Cr(VI) ions from synthetic wastewater containing 20 mg/L Cr(VI) with an adsorbent dosage 2 g/L in strong acidic conditions pH = 2 and T = 30°C.
- Adsorption kinetics followed a second-order rate expression. Adsorption equilibrium data of Cr(VI) was best described by Langmuir and Dubinin–Radushkevich isotherm models based on linearized correlation coefficients.
- Chromium(VI) adsorption onto RS exhibited spontaneous and endothermic processes as indicated by the thermodynamic parameters. The positive value of the entropy change, suggests the increased randomness.

Statements and declarations

Funding

The authors declare that no funds, grants, or other support were received during the preparation of this manuscript.

Competing interests

The authors have no relevant financial or non-financial interests to disclose.

Author contributions

All authors contributed to the study conception and design. Material preparation, data collection and analysis were performed by Cherifi Mouna. The first draft of the manuscript was written by Cherifi Mouna and Mecibah Wahiba. Data of material analysis was interpreted by Cherifi Mouna, Mecibah Wahiba and Bouasla Souad. Debra F. Laefer: checked the paper's results and English and aided in the substance and form of the revisions. Hazourli Sabir: Validation, review & editing, visualization, and supervision

Data availability

All data generated or analysed during this study are included in this published article

Novelty statement

The main objective of this paper was to find low cost-effective adsorbent. Sewage sludge was analyzed and tested to adsorb toxic Cr(VI). Obtained results shows that sludge could be an effective adsorbent.

Acknowledgments

- Acknowledgment to express for the below institutions for their assistance to accomplish this work:
- Unit research of emerging materials Setif. Algeria.
- Research center in industrial technologies. CRTI. PO. BOX 64 Cheraga 15014 Algeria.
- Laboratory of Applied Mechanics of New Materials. University of 08 Mai 1945 Guelma. Algeria.

References

[1] H. Cheng, T. Zhou, Q. Li, L. Lu, C. Lin, Anthropogenic chromium emissions in China from 1990 to 2009, PLoS One, 9 (2014) e87753, doi: 10.1371/journal.pone.0087753.
[2] J. Kotaś, Z. Stasicka, Chromium occurrence in the environment and methods of its speciation, Environ. Pollut., 107 (2000) 263–283.
[3] Asmatullah, S.N. Qureshi, A.R. Shakoori, Hexavalent chromium-induced congenital abnormalities in chick embryos, J. Appl. Toxicol., 18 (1998) 167–171.
[4] IARC Monographs on the Evaluation of Carcinogenic Risks to Humans: Chromium, Nickel and Welding, Volume 49, IARC, Lyon, France, 1990.
[5] L.E. Eary, D. Rai, Chromate removal from aqueous wastes by reduction with ferrous ion, Environ. Sci. Technol., 22 (1988) 972–977.
[6] M. Faisal, S. Hasnain, Bacterial Cr(VI) reduction concurrently improves sunflower (*Helianthus annuus* L.) growth, Biotechnol. Lett., 27 (2005) 943–947.
[7] L.-Y. Chang, Alternative chromium reduction and heavy metal precipitation methods for industrial wastewater, Environ. Prog., 22 (2003) 174–182.
[8] S.-S. Chen, C.-Y. Cheng, C.-W. Li, P.-H. Chai, Y.-M. Chang, Reduction of chromate from electroplating wastewater from pH 1 to 2 using fluidized zero valent iron process, J. Hazard. Mater., 142 (2007) 362–367.

[9] M.C. Fournier-Salaün, C. Vauclair, Recovery of chromique ions from aqueous effluents by liquid membrane in continuous mode, Desalination, 144 (2002) 227–229.
[10] S. Nezar, Y. Cherifi, A. Barras, A. Addad, E. Dogheche, N. Saoula, N. Aïcha Laoufi, P. Roussel, S. Szunerits, R. Boukherroub, Efficient reduction of Cr(VI) under visible light irradiation using CuS nanostructures, Arabian J. Chem., 12 (2019) 215–224.
[11] M. Cherifi, S. Hazourli, S. Pontvianne, J.-P. Leclerc, F. Lapicque, Electrokinetic removal of aluminum and chromium from industrial wastewater electrocoagulation treatment sludge, Desal. Water Treat., 57 (2016) 18500–18515.
[12] B. Mukhopadhyay, J. Sundquist, R.J. Schmitz, Removal of Cr(VI) from Cr-contaminated groundwater through electrochemical addition of Fe(II), J. Environ. Manage., 82 (2007) 66–76.
[13] C.M. Stern, T.O. Jegede, V.A. Hulse, N. Elgrishi, Electrochemical reduction of Cr(VI) in water: lessons learned from fundamental studies and applications, Chem. Soc. Rev., 50 (2021) 1642–1667.
[14] V. Dimos, K.J. Haralambous, S. Malamis, A review on the recent studies for chromium species adsorption on raw and modified natural minerals, Crit. Rev. Env. Sci. Technol., 42 (2012) 1977–2016.
[15] M. Owlad, M.K. Aroua, W.A.W. Daud, S. Baroutian, Removal of hexavalent chromium-contaminated water and wastewater: a review, Water Air Soil Pollut., 200 (2009) 59–77.
[16] M. Rafatullah, S. Othman, H. Rokiah, A. Anees, Adsorption of methylene blue on low-cost adsorbents: a review, J. Hazard. Mater., 177 (2010) 70–80.
[17] D. Mohan, C.U. Pittman Jr., Activated carbons and low cost adsorbents for remediation of tri- and hexavalent chromium from water, J. Hazard. Mater., 137 (2006) 762–811.
[18] X. Dong, L.Q. Ma, Y. Li, Characteristics and mechanisms of hexavalent chromium removal by biochar from sugar beet tailing, J. Hazard. Mater., 190 (2011) 909–915.
[19] D. Fytili, A. Zabaniotou, Utilization of sewage sludge in EU application of old and new methods—a review, Renewable Sustainable Energy Rev., 12 (2008) 116–140.
[20] L.Y. Deng, G.R. Xu, Z.C. Yan, Q.H. Liu, G.B. Li, Removal effect of Cr(VI) by adsorbent made from sewage sludge, Water Sci. Technol., 62 (2010) 2961–2969.
[21] Y. Li, X. Chen, L. Liu, P. Liu, Z. Zhou, Huhetaoli, Y. Wu, T. Lei, Characteristics and adsorption of Cr(VI) of biochar pyrolyzed from landfill leachate sludge, J. Anal. Appl. Pyrolysis, 162 (2022) 105449, doi: 10.1016/j.jaap.2022.105449.
[22] T. Chen, Z. Zhou, S. Xu, H. Wang, W. Lu, Adsorption behavior comparison of trivalent and hexavalent chromium on biochar derived from municipal sludge, Bioresour. Technol., 190 (2015) 388–394.
[23] C. Tan, Z. Zeyu, X. Sai, W. Hongtao, L. Wenjing, Adsorption behavior comparison of trivalent and hexavalent chromium on biochar derived from municipal sludge, Bioresour. Technol., 190 (2015) 388–394.
[24] F. Gorzin, M. Bahri Rasht Abadi, Adsorption of Cr(VI) from aqueous solution by adsorbent prepared from paper mill sludge: kinetics and thermodynamics studies, Adsorpt. Sci. Technol., 36 (2018) 149–169.
[25] X. Qi, E. Zhou, X. Wu, S. Luo, Y. Song, Preparation of adsorbent by pyrolysis of sludge mixed with steel slag and study on adsorption of chromium ion in water, Front. Energy Res., (2022) 914, doi: 10.3389/fenrg.2021.771603.
[26] M. Schreier, T.E. Feltes, M.T. Schaal, J.R. Regalbuto, The determination of oxide surface charging parameters for a predictive metal adsorption model, J. Colloid Interface Sci., 348 (2010) 571–578.
[27] M. Kosmulski, The pH dependent surface charging and points of zero charge. VI. Update, J. Colloid Interface Sci., 426 (2014) 209–212.
[28] M. Benjelloun, Y. Miyah, G. Akdemir Evrendilek, F. Zerrouq, S. Lairini, Recent advances in adsorption kinetic models: their application to dye types, Arabian J. Chem., 14 (2021) 103031, doi: 10.1016/j.arabjc.2021.103031.
[29] S. Afroze, T.K. Sen, H.M. Ang, Adsorption removal of zinc(II) from aqueous phase by raw and base modified *Eucalyptus sheathiana* bark: kinetics, mechanism and equilibrium study, Process Saf. Environ. Prot., 102 (2016) 336–352.
[30] H. Moussout, H. Ahlafi, M. Aazza, H. Maghat, Critical of linear and nonlinear equations of pseudo-first-order and pseudo-second-order kinetic models, Karbala Int. J. Mod. Sci., 4 (2018) 244–254.
[31] M.A. Salam, R.M. El-Shishtawy, A.Y. Obaid, Synthesis of magnetic multi-walled carbon nanotubes/magnetite/chitin magnetic nanocomposite for the removal of Rose Bengal from real and model solution, J. Ind. Eng. Chem., 20 (2014) 3559–3567.
[32] T.D. Çiftçi, E. Henden, Nickel/nickel boride nanoparticles coated resin: a novel adsorbent for arsenic(III) and arsenic(V) removal, Powder Technol., 269 (2015) 470–480.
[33] Y. Ho, Review of second-order models for adsorption systems, J. Hazard. Mater., 136 (2006) 681–689.
[34] W.J. Weber, J.C. Morris, Kinetics of adsorption on carbon from solution, Sanit. Eng. Resolut. Div., 89 (1963) 31–59.
[35] A.O. Babatunde, Y.Q. Zhao, Equilibrium and kinetic analysis of phosphorus adsorption from aqueous solution using waste alum sludge, J. Hazard. Mater., 184 (2010) 746–752.
[36] S. Bounit, M. El Meray, A. Chehbouni, Influence du traitement thermique sur quatre éléments métalliques (Cu, Cd, Pb et Zn) des boues résiduaires, Afr. Sci., 1 (2005) 69–80.
[37] J.A.G. Gomes, P. Daida, M. Kesmez, M. Weir, H. Moreno, J.R. Parga, G. Irwin, H.M. Whinney, T. Grady, E. Peterson, D.L. Cocke, Arsenic removal by electrocoagulation using combined Al–Fe electrode system and characterization of products, J. Hazard. Mater., 139 (2007) 220–231.
[38] A.K. Golder, A.N. Samanta, S. Ray, Removal of phosphate from aqueous solutions using calcined metal hydroxides sludge waste generated from electrocoagulation, Sep. Purif. Technol., 52 (2006) 102–109.
[39] Z. Ren, X. Xu, X. Wang, B. Gao, Q. Yue, W. Song, L. Zhang, H. Wang, FTIR, Raman, and XPS analysis during phosphate, nitrate and Cr(VI) removal by amine cross-linking biosorbent, J. Colloid Interface Sci., 468 (2016) 313–323.
[40] D. Özçimen, A. Ersoy-Meriçboyu, Characterization of biochar and bio-oil samples obtained from carbonization of various biomass materials, Renewable Energy, 35 (2010) 1319–1324.
[41] X.S. Wang, L.F. Chen, F.Y. Li, K.L. Chen, W.Y. Wan, Y.J. Tang, Removal of Cr(VI) with wheat-residue derived black carbon: reaction mechanism and adsorption performance, J. Hazard. Mater., 175 (2010) 816–822.
[42] B.D. Zdravkov, J.J. Čermák, M. Šefara, J. Janků, Pore classification in the characterization of porous materials: a perspective, Cent. Eur. J. Chem., 5 (2007) 385–395.
[43] Z.H. Hu, M.P. Srinivasan, Y.M. Ni, Novel activation process for preparing highly microporous and mesoporous activated carbons, Carbon, 39 (2001) 877–886.
[44] X. Wang, N. Zhu, B. Yin, Preparation of sludge-based activated carbon and its application in dye wastewater treatment, J. Hazard. Mater., 153 (2008) 22–27.
[45] S. Payel, Md. A. Hashem, Md. A. Hasan, Recycling biochar derived from tannery liming sludge for chromium adsorption in static and dynamic conditions, Environ. Technol. Innovation, 42 (2021) 102010, doi: 10.1016/j.eti.2021.102010.
[46] S.H. Hu, S.C. Hu, Pyrolysis of paper sludge and utilization for ionic dye adsorption, BioResources, 8 (2013) 1028–1042
[47] J. Wu, H. Zhang, P.J. He, Q. Yao, L.-M. Shao, Cr(VI) removal from aqueous solution by dried activated sludge biomass, J. Hazard. Mater., 176 (2010) 697–703.
[48] A. Hadfi, S.B. Aazza, M. Belattar, S. Mohareb, A. Driouiche, Study of the physico-chemical quality of the water of irrigation in Biougra circle along with highlighting the effectiveness of an inhibitor of calcium carbonate precipitation, Mediterr. J. Chem., 7 (2018) 272, doi: 10.13171/mjc74181121-hadfi.
[49] M.M. Tang, R. Bacon, Carbonization of cellulose fibers—I. Low temperature pyrolysis, Carbon, 2 (1964) 211–220.
[50] A. Magdziarz, M. Wilk, Thermogravimetric study of biomass, sewage sludge and coal combustion, Energy Convers. Manage., 75 (2013) 425–430.
[51] V.K. Gupta, T.A. Saleh, Sorption of pollutants by porous carbon, carbon nanotubes and fullerene-an overview, Environ. Sci. Pollut. Res., 20 (2013) 2828–2843.

[52] M.A.M. Salleh, D.K. Mahmoud, W.A.W.A. Karim, A. Idris, Cationic and anionic dye adsorption by agricultural solid wastes: a comprehensive review, Desalination, 280 (2011) 1–13.
[53] B. Kakavandi, R.R. Kalantary, M. Farzadkia, A.H. Mahvi, A. Esrafili, A. Azari, A.R. Yari, A.B. Javid, Enhanced chromium(VI) removal using activated carbon modified by zero valent iron and silver bimetallic nanoparticles, J. Environ. Health Sci. Eng., 12 (2014) 115, doi: 10.1186/s40201-014-0115-5.
[54] N.Y. Mezenner, A. Bensmaili, Kinetics and thermodynamic study of phosphate adsorption on iron hydroxide-eggshell waste, J. Chem. Eng., 147 (2009) 87–96.
[55] Y.S. Ho, C.C. Chiang, Sorption studies of acid dye by mixed sorbents, Adsorption, 7 (2001) 139–147.
[56] S. Kara, C. Aydiner, E. Demirbas, M. Kobya, N. Dizge, Modeling the effects of adsorbent dose and particle size on the adsorption of reactive textile dyes by fly ash, Desalination, 212 (2007) 282–293.
[57] J.L. Arias, M.S. Fernandez, J.E. Dennis, A.I. Caplan, Collagens of the chicken eggshell membranes, Connect. Tissue Res., 26 (1991) 37–45.
[58] P. Regmi, J.L. Garcia Moscoso, S. Kumar, X. Cao, J. Mao, G. Schafran, Removal of copper and cadmium from aqueous solution using switchgrass biochar produced via hydrothermal carbonization process, J. Environ. Manage., 109 (2012) 61–69.
[59] I.M. Trifi, Étude de l'élimination du chrome VI par adsorption sur l'alumine activée par dialyse ionique croisée, Phd Thesis, Université Paris-Est, 2012.
[60] A. Attia, S. Khedr, S. Elkholy, Adsorption of chromium ion(VI) by acid activated carbon, Braz. J. Chem. Eng., 27 (2010) 183–193.
[61] M. Zhang, Z. Zhang, Y. Peng, L. Feng, X. Li, C. Zhao, K. Sarfaraz, Novel cationic polymer modified magnetic chitosan beads for efficient adsorption of heavy metals and dyes over a wide pH range, Int. J. Biol. Macromol., 156 (2020) 289–301.
[62] J. Wu, H. Zhang, P.J. He, Q. Yao, L.M. Shao, Cr(VI) removal from aqueous solution by dried activated sludge biomass, J. Hazard. Mater., 176 (2010) 697–703.
[63] M. Nahid, M.H.I. Genawi, H.E. Muftah, E.A. Awad, Chromium removal from tannery wastewater by electrocoagulation: optimization and sludge characterization, Water, 12 (2020) 1374, doi: 10.3390/w12051374.
[64] Y. Li, X. Hu, X. Liu, Y. Zhang, Q. Zhao, P. Ning, S. Tian, Adsorption behavior of phenol by reversible surfactant-modified montmorillonite: mechanism, thermodynamics, and regeneration, J. Chem. Eng., 334 (2018) 1214–1221.
[65] İ. Tosun, Ammonium removal from aqueous solutions by clinoptilolite: determination of isotherm and thermodynamic parameters and comparison of kinetics by the double exponential model and conventional kinetic models, Int. J. Environ. Res. Public Health, 9 (2012) 970–984.
[66] K. Vijayaraghavan, T. Padmesh, K. Palanivelu, M. Velan, Biosorption of nickel(II) ions onto *Sargassum wightii*: application of two-parameter and three-parameter isotherm models, J. Hazard. Mater., 133 (2006) 304–308.
[67] M.A.H. Dhaif-Allah, S.N. Taqui, U.T. Syed, A.A. Syed, Kinetic and isotherm modeling for acid blue 113 dye adsorption onto low-cost nutraceutical industrial fenugreek seed spent, Appl. Water Sci., 10 (2020) 58, doi: 10.1007/s13201-020-1141-3.
[68] M.R.R. Kooh, L.B.L. Lim, L.H. Lim, M.K. Dahri, Separation of toxic rhodamine B from aqueous solution using an efficient low-cost material, *Azolla pinnata*, by adsorption method, Environ. Monit. Assess., 188 (2016) 108, doi: doi: 10.1007/s10661-016-5108-7.
[69] A.A. Inyinbor, F.A. Adekola, G.A. Olatunji, Kinetics, isotherms and thermodynamic modeling of liquid phase adsorption of Rhodamine B dye onto *Raphia hookerie* fruit epicarp, Water Resour. Ind., 15 (2016) 14–27.
[70] S. Mullerova, E. Baldikova, J. Prochazkova, K. Pospiskova, I. Safarik, Magnetically modified macroalgae *Cymopolia barbata* biomass as an adsorbent for safranin O removal, Mater. Chem. Phys., 225 (2019) 174–180.
[71] S.R. Sumanjit, R.K. Mahajan, Equilibrium, kinetics and thermodynamic parameters for adsorptive removal of dye Basic Blue 9 by ground nut shells and *Eichhornia*, Arabian J. Chem., 9 (2016) S1464–S1477.
[72] M. Abbas, Removal of brilliant green (BG) by activated carbon derived from medlar nucleus (ACMN) – kinetic, isotherms and thermodynamic aspects of adsorption, Adsorpt. Sci. Technol., 38 (2020) 464–482.
[73] P. Jain, K. Sahoo, L. Mahiya, H. Ojha, H. Trivedi, A.S. Parmar, M. Kumar, Color removal from model dye effluent using PVA-GA hydrogel beads, J. Environ. Manage., 281 (2021) 111797, doi: 10.1016/j.jenvman.2020.111797.
[74] J.O. Ojediran, A.O. Dada, S.O. Aniyi, R.O. David, A.D. Adewumi, Mechanism and isotherm modeling of effective adsorption of malachite green as endocrine disruptive dye using acid functionalized maize cob (AFMC), Sci. Rep., 11 (2021), doi: 10.1038/s41598-021-00993-1.
[75] E.O. Oyelude, J.A.M. Awudza, S.K. Twumasi, Equilibrium, kinetic and thermodynamic study of removal of eosin yellow from aqueous solution using teak leaf litter powder, Sci Rep, 7 (2017) 12198, doi: 10.1038/s41598-017-12424-1.
[76] M.P. Tavlieva, S.D. Genieva, V.G. Georgieva, L.T. Vlaev, Kinetic study of brilliant green adsorption from aqueous solution onto white rice husk ash, J. Colloid Interface Sci., 409 (2013) 112–122.
[77] I. Tsibranska, E. Hristova, Comparison of different kinetic models for adsorption of heavy metals onto activated carbon from apricot stones, Bulg. Chem. Commun., 43 (2011) 370–377.
[78] P. Senthil Kumar, C. Senthamarai, A. Durgadevi, Adsorption kinetics, mechanism, isotherm, and thermodynamic analysis of copper ions onto the surface modified agricultural waste, Environ. Prog. Sustainable Energy, 33 (2014) 28–37.
[79] Y.S. Shen, S.L. Wang, Y.M. Tzou, Y.Y. Yan, W.H. Kuan, Removal of hexavalent Cr by coconut coir and derived chars – the effect of surface functionality, BioTechnology, 104 (2012) 165–172.
[80] P.T. de Souza E Silva, N.T. de Mello, M.M.M. Duarte, M. Conceição, B.S.M. Montenegro, A.N. Araújo, B. de Barros Neto, V.L. da Silva, Extraction and recovery of chromium from electroplating sludge, J. Hazard. Mater., 128 (2006) 39–43.
[81] A. Chaudhary, B. Ganguli, S.M. Grimes, The use of chromium waste sludge for the adsorption of colour from dye effluent streams, J. Chem. Technol. Biotechnol., 77 (2002) 767–770.
[82] C.K. Lee, K.S. Low, S.W. Chow, Chrome sludge as an adsorbent for colour removal, Environ. Technol., 17 (1996) 1023–1028.
[83] L. Liu, X. Liu, D. Wang, H. Lin, L. Huang, Removal and reduction of Cr(VI) in simulated wastewater using magnetic biochar prepared by co-pyrolysis of nano-zero-valent iron and sewage sludge, J. Cleaner Prod., 257 (2020) 120562, doi: 10.1016/j.jclepro.2020.120562.
[84] J. Wang, R. Cao, D. He, A. Saleem, Facile preparation of polyethyleneimine modified activated sludge-based adsorbent for hexavalent chromium removal from aqueous solution, Sep. Sci. Technol., 56 (2021) 498–506.